ELSEVIER

Journal of Power Sources 80 (1999) 226–234

JOURNAL OF POWER SOURCES

Comparative studies of polymer electrolyte membrane fuel cell stack and single cell

Deryn Chu *, Rongzhong Jiang

U.S. Army Research Laboratory, Electrochemistry Branch, Sensor and Electronic Devices Directorate, Mail Stop AMSRL-SE-DC, Adelphi, MD 20783-1197, USA

Abstract

The polymer electrolyte membrane fuel cell (PEMFC) was investigated comparatively as a single cell and a 30-cell stack. Various types of Nafion membranes, such as Nafion 117, 115, 112 and 105, were tested as electrolyte within the single cell and at different temperatures, among which Nafion 112 gave the optimal result. The 30-cell stack was evaluated at different humidities and temperatures. The potential–current and power–current curves, both for single cell and the stack, were analyzed by computer simulation, whereby the kinetic and mass-transfer parameters were calculated. The long-term performance of the stack and the water production during long-term operation were also measured.

Keywords: Fuel cells; Polymer electrolyte membrane

1. Introduction

Because of its lightweight, high-energy, high-power, non-emission and low-temperature-operation, the polymer electrolyte membrane fuel cell (PEMFC) has received much attention in recent years [1–10]. The research and development of materials, catalysts, and electrode components for single cells has made significant progress during last decade. To meet the requirement of practical applications a large number of single cells are assembled together, and known as a PEMFC stack. Most recently, more and more PEMFC stacks were developed with a variety of types and functions [11–14]. The performance of a PEMFC stack is different from that of a single PEMFC cell. The PEMFC stack has much higher operating voltage and stronger power and better fuel-energy efficiency. Our curiosity is to explore what differences there are in the electrochemical performance between PEMFC stacks and single cells, and to attempt to promote the practical applications of PEMFC stacks in both military and civilian portable power sources.

In the present paper we make a comparative study of the PEMFC single cell and stack. For the single cell we emphasize the important role of different Nafion membranes in the construction of PEMFC's membrane-electrode assembly (MEA), while for the stack we evaluate the performance of a 100 W PEMFC stack consisting of 30 cells, concentrating on kinetic and mass-transfer electrode processes.

2. Experimental

2.1. Construction of the PEMFC single cell

Various Nafion membranes (numbered as 105, 112, 115, 117) were obtained from Du Pont Chemical. They were soaked in a mixture of H_2O_2/H_2O at approximately 80°C for 2 h. After the Nafion membranes became transparent they were washed with distilled water, followed by soaking and boiling in a 1 M H_2SO_4 solution for 2 h. Water rinsing again was the last step, to remove excess H_2SO_4, and the film, being ready to use, was stored in distilled water.

The commercially available electrocatalyst, 20% platinum on Vulcan XC-72 carbon (from E-Tek), was suspended in an aqueous Nafion solution, then the mixture was sonicated using an ultrasonic bath. The final electrocatalyst–Nafion mixture was sprayed on to a Tory carbon paper. The amount of Pt and Nafion on the electrode were about 0.4 and 0.5 mg cm^{-2}, respectively. The membrane-

* Corresponding author. Tel.: +1-301-721-3451; Fax: +1-301-721-3402; E-mail: dchu@arl.mil

0378-7753/99/$ - see front matter
PII: S0378-7753(98)00263-8

electrode assembly (MEA), a key component of the PEMFC system, is a proton conducting membrane such as Nafion, laminated between the active sites of two electrodes (carbon supported platinum black). MEA is assembled conventionally, using a hot pressing process conducted at 140°C and 8.3 MPa (1200 psi) for 90 s, in which the electrode–membrane–electrode laminate is heated until the glass-transition temperature of the membrane is reached. Two titanium plates with fine gas-passing channels on their inner sides to the MEA were used to hold the MEA as a single cell. Pure hydrogen was fuel and pure oxygen was oxidant. A Hewlett-Packard electronic load (Model No. 6050A) and a Hewlett-Packard multimeter were used to measure the single cell's current and voltage, respectively.

2.2. Construction of the 30-cell PEMFC stack

The self-humidifying, 100 W, PEMFC stack comprised 30, series-connected, cells. The area of each electrode was approximately 60 cm^2, and the open-circuit voltage approximately 30. The air was supplied to the cathode by an electric fan, and another electric fan was used for cooling the stack. The self-humidifying function was obtained by blowing input air through a small chamber wherein water was collected from the stack's cathodes. High purity hydrogen (99.99%) was used. The environmental temperature and humidity of the stack were controlled with a Tenney Environment Chamber (model No. BTRC)—which was programmed through a computer with Linktenn II Software—and a Heatless Dryer (model No. HF 200A). An Arbin battery tester BT-2043 was used for program-controlled experiments on the PEMFC stack. In order to get reproducible results, all experiments within the Tenney Environment Chamber for the PEMFC stack were carried out after constancy of temperature and humidity had been reached for more than 6 h.

3. Results and discussion

3.1. Performance of a single cell

3.1.1. Effect of different Nafion membranes

Fig. 1 shows the polarization curves of a PEMFC single cell with different MEAs. These are typical of results for hydrogen/oxygen fuel cells. The initial drop of the potential–current curve is due to an electrochemical activation process, which is caused by the sluggish kinetics of oxygen reduction at the cathode electrode surface. On the other hand, the linear decrease of the potential–current curves with increasing load current density is due to ohmic polarization, which is attributed to the ion-flow through the electrolyte membrane and the electron flow through the electrode materials. These results have demonstrated that the current density is significantly enhanced when the membrane thickness is decreased from 7 mil (0.175 mm, Nafion 117) to 2 mil (Nafion 112).

For Nafion membranes 112, 105, 115 and 117, the values of the current density of the single cell at 0.72 V were approximately 1.0, 0.6, 0.5 and 0.4 A cm^{-2}, respectively. Apparently, Nafion 112 membrane gave the optimal performance. The kinetic parameters can be obtained by computer simulation using the following empirical equations:

$$E_i = E_0 - b \log i - Ri \quad (1)$$

$$E_0 = E_r + b \log i_0 \quad (2)$$

$$E_i = E_0 - b \log i - Ri - i_m \mathrm{m} \exp[ni_m] \quad (3)$$

$$i_m = i - i_d \qquad (\text{when } i > i_d) \quad (4)$$

$$i_m = 0 \qquad (\text{when } i \le i_d) \quad (5)$$

where E_i and i are the experimentally measured potential and current, E_r is the reversible potential for the cell, i_o and b are the exchange current and the Tafel slope for the

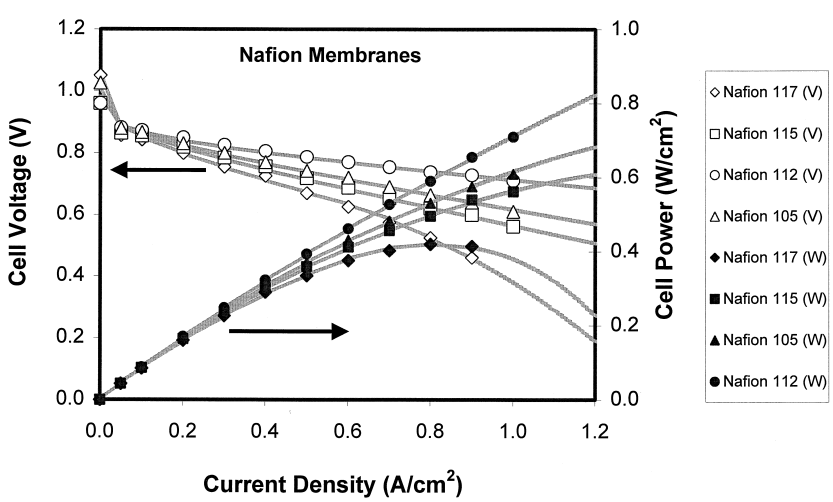

Fig. 1. Polarization curves of a single cell with different grades of Nafion. The points are experimental data and the lines were computed from an empirical equation.

oxygen reduction, respectively. R represents the d.c. resistance, such as resistances in the polymer membrane and other electrode components, which causes the linear variation of potential with current shown above. Here, i_d is the minimum value of current that causes the voltage deviation from the linearity at the higher current range. The i_d value can be obtained from the experimental curve and from the calculated curve using Eq. (1). Hence Eq. (1) can be used to describe the electrochemical process, which is controlled only by activation and ohmic polarization, while Eq. (3) can be used to describe the entire electrochemical process including activation, ohmic and mass-transfer.

For the Nafion membranes 105, 112 and 115 there was no apparent mass-transfer process, because no deviation from linearity was observed at the high current ranges of these curves. However, when Nafion 117 was used as membrane, the curve is slightly bent downwards at the high current density range signaling the existence of a mass-transfer process.

In Fig. 1 the points were obtained from experiments and the lines were simulated from Eq. (1) (for Nafion 105, 112, 115) or from Eq. (3) (for Nafion 117). The single cell's kinetic and mass-transfer parameters for different Nafion membranes are shown in Table 1.

The value of E_0 does not change significantly for different Nafion membranes. It is interesting that the b and R values decrease in the order of Nafion 117, 115, 105 and 112. The power–current curves are also shown in Fig. 1. Peak power is observed at about 0.9 A cm^{-2} on the power–current curve for Nafion 117. For other Nafion membranes no peak in the power curve was observed. The simulated curves can be used to predict the single cells' performance beyond the range of the experimental data. For example, at current density as 1.2 A/cm^2, estimated power densities for Nafion 112, 105, 115 and 117 are 0.82, 0.68, 0.61 and 0.23 W cm^{-2}, respectively.

Table 1
Electrode kinetic and mass transfer parameters at 50°C, calculated from the polarization curves for the PEMFC single cell with different Nafion electrolyte membranes

Nafion number	E_0, V	b, mV dec^{-1}	R, Ω cm^2	m, Ω cm^2	n, A^{-1} cm^2	i_d, A cm^{-2}
112	0.99	56.0	0.11	–	–	–
105	1.00	58.0	0.21	–	–	–
115	1.01	62.0	0.26	–	–	–
117	1.02	68.0	0.33	0.18	0.15	0.65

3.1.2. Effect of temperature

Because of its optimal performance, the Nafion 112 membrane was selected for further study at various temperatures. Fig. 2 shows the potential–current and power–current curves for Nafion 112 membrane in the MEA at various temperatures. Usually, a single cell has good heat exchange with the local environment. Therefore, the inner temperature and the environmental temperature can be considered the same for the single cell (this is not the case for a stack). The single cell's potential increases with temperature from 24 to 50°C and so does the power at the same current density. At higher temperatures, the ionic conductivity of the Nafion membrane is enhanced and the rate of both electrode reactions is faster. So, it seems that higher temperatures should be better for the operation of a single cell. However, further increase in temperature would cause dehydration of the membrane, resulting in reduced conductivity and inferior cell performance.

From the simulated curves in Fig. 2, one can deduce that the cell voltages and powers at a current density of 1.4 A cm^{-2} will be 0.51, 0.60, 0.66 V and 0.72, 0.84 0.92 W cm^{-2} at 24, 40 and 50°C, respectively. The electrode's kinetic parameters at different temperatures for the single cell using Nafion 112 as membrane are summarized in Table 2. The parameters of b and E_0 seem to show no

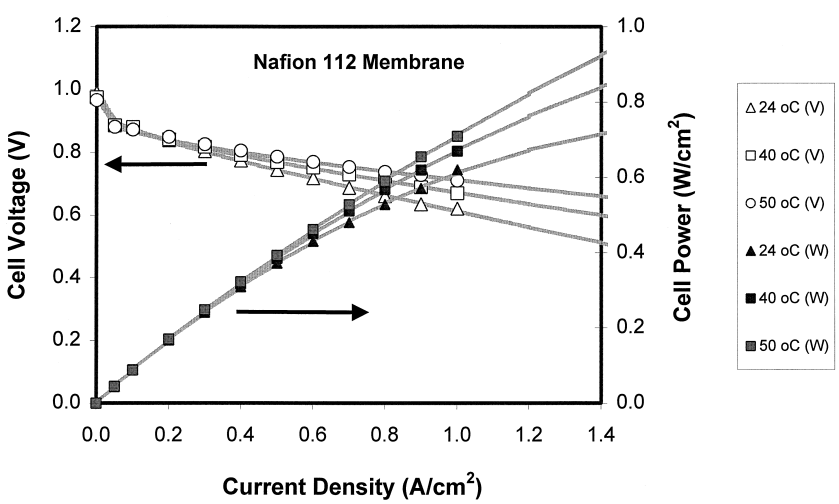

Fig. 2. Electrochemical performance at various temperatures of MEAs using Nafion 112. The points are experimental data and the lines were computed from an empirical equation.

Table 2
Electrode kinetic parameters at different temperatures, calculated from the polarization curves for the PEMFC single cell with Nafion 112 as electrolyte membrane

Temperature, °C	E_0, V	R, Ω cm^2	b, mV dec^{-1}
24	1.01	0.23	56.0
40	1.00	0.16	56.0
50	0.99	0.11	56.0

significant difference, however, R is getting smaller with increase of temperature because the ionic conductance of the membrane electrolyte is improved at the elevated temperatures.

3.2. Performance of the PEMFC stack

3.2.1. Polarization curves

Fig. 3 shows the potential–current and power–current curves at room temperature (ca. 20°C) and room humidity conditions (ca. 70% r.h.). of a 30-cell PEMFC stack. The shape of both curves differ little from those for the single cell, except for the much higher open circuit potential (about 30 times that of the single cell) and much higher power output. The points on the curves were obtained from experiment, and the lines from simulation, using Eq. (1).

Up to a current of 7 A there is no curving down of the measured potential–current curve, and the data fit to Eq. (1) is good. The electrode process is activation and ohmic controlled within this current range.

Because the stack is composed of 30 cells, the heat-equilibrium inside the stack is hard to reach. Therefore, the temperature gradient from the interior of the stack to the external environment is significant and is also time-dependent. This feature makes the evaluation of PEMFC stacks more difficult than that of a single cell. Because heat produced at the inner stack cannot be dissipated quickly, the inside and outside temperature of the stack may vary up to more than 26°C, depending on the experimental conditions. At 7 A, the voltage and power of the stack are 19.8 V and 140 W, respectively. From the simulated curves one can see that, if the current is extended to 10 A, the voltage and power will be 18.3 V and 183 W. The electrode kinetic parameters are also obtained from the simulation, which are shown in Table 3. Here, values for E_0, b and R should be, and are, 30 times the average value for a single cell, whose averages for E_0, b and R are 1.07 V, 83 mV dec^{-1} and 0.013 Ω.

Surprisingly, with this 100 W PEMFC stack, we obtained more than 140 W at 7 A, with the computed performance of the stack reaching 180 W at 10 A. These results demonstrate that the PEMFC stack performs more advantageously than a single cell.

3.2.2. Effect of humidity

Although the 30-cell PEMFC stack is designed with a self humidifying function, we still needed to evaluate the effect of relative humidity (% r.h.) on the stack's performance. The PEMFC stack was put into a Tenney environmental chamber, where the temperature and humidity were controlled automatically. Fig. 4 shows the potential–current and power–current curves for the PEMFC stack with different humidities and at a constant temperature of 30°C. The humidity was varied in steps—10%, 30%, 50%, 70% and 90% r.h. (for reason of clarity, only 10% and 90% r.h. results are included in Fig. 4).

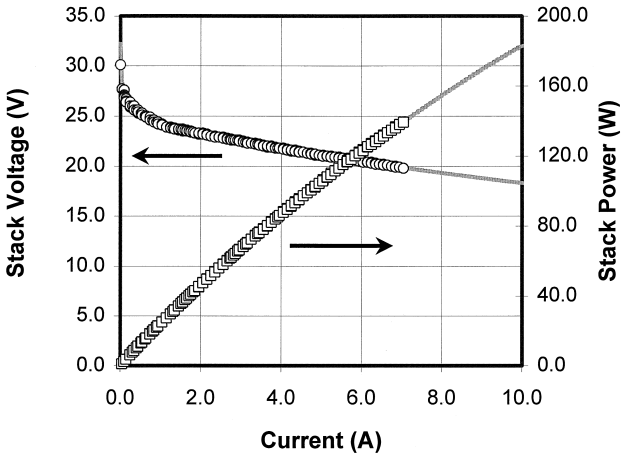

Fig. 3. Polarization behaviour of the 100 W PEMFC stack at room temperature (ca. 20°C) and room humidity (ca. 70% r.h.). The points are experimental data and the lines were computed from an empirical equation.

As expected, the potential–current and power–current curves for 10% and 90% r.h. show only a slight difference. Here, the self-humidifying function plays an important role. It is observed in Fig. 4 that the potential–current curves are bent down slightly at the higher current range, which indicates that a mass-transfer process is occurring. An excellent experimental data fit has been obtained with Eq. (3) producing the simulated data, shown as lines in Fig. 4. Computed peak powers at 10% and 90% r.h. are 146.0 W at 9.0 A and 167.4 W at 10.1 A, respectively. The kinetic and mass-transfer parameters are obtained from simulation, and shown in Table 3.

For a humidity change from 10% to 90% r.h., the parameters of E_0, b and R only change slightly. The n value, which describes the degree of curvature on poten-

Table 3
Electrode-kinetic and mass-transfer parameters for the 100 W PEMFC stack at different humidities and at a constant temperature of 30°C

% r.h.	E_0, V	b, mV dec^{-1}	R, Ω	m, Ω	n, A^{-1}	i_d, A
90	31.5	1900	0.37	0.31	0.15	4.54
10	31.0	1900	0.39	0.36	0.15	4.04
Room*	32.2	2500	0.39	–	–	–

* Relative humidity ca. 70% r.h. at a room temperature of ca. 20°C.

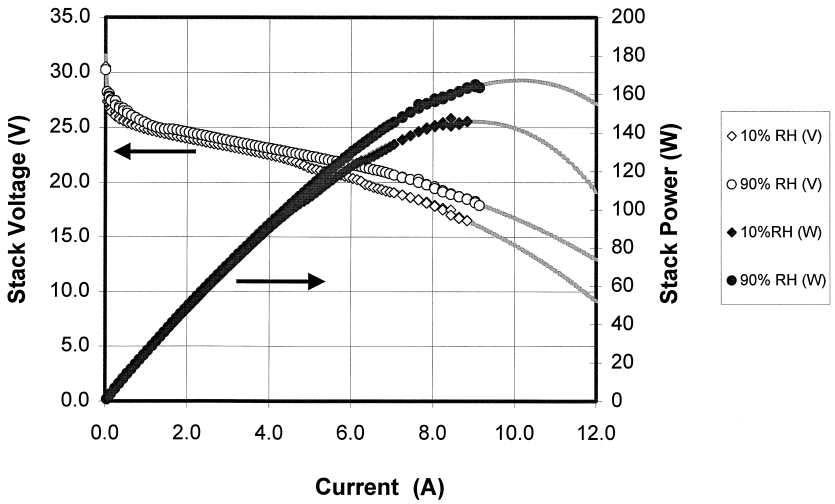

Fig. 4. Effect of relative humidity on the operating voltage and power output of the 100 W PEMFC stack at a constant temperature of 30°C. The points are experimental data and the extrapolated curves were computed from an empirical equation.

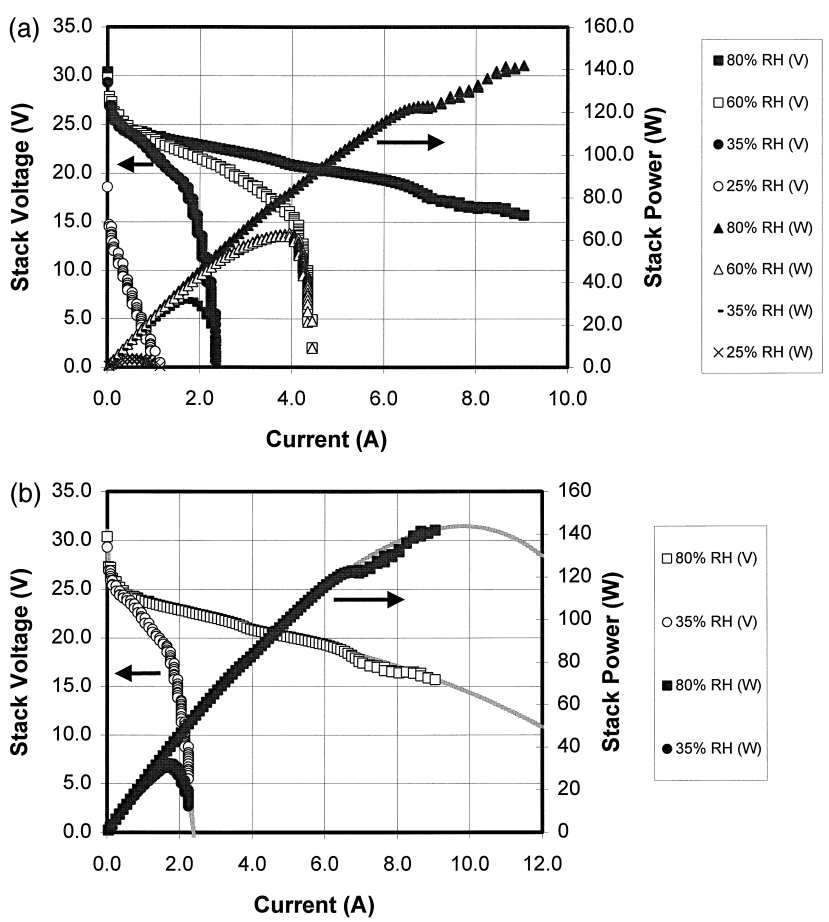

Fig. 5. (a) Effect of relative humidity on the operating voltage and power output of the 100 W PEMFC stack at a constant temperature of 10°C. (b) Effect of relative humidity on the operating voltage and power output of the 100 W PEMFC stack at a constant temperature of 10°C, whereas the points are experimental data and the extrapolated curves were computed from an empirical equation.

Table 4
Electrode-kinetic and mass-transfer parameters for the 100 W PEMFC stack at different humidities and at a constant temperature of 10°C

% r.h.	E_0, V	b, mV dec^{-1}	R, Ω	m, Ω	n, A^{-1}	i_d, A
80	30.5	2050	0.48	0.19	0.15	3.64
35	31.0	2150	2.40	0.46	2.50	1.04

tial–current curves at higher currents, is very small, ca. 0.15, for both low and high humidities (10% and 90% r.h.). The i_d value is larger and the m value is smaller at 90% than that at 10% r.h. Apparently, the stack performance at the higher humidity condition is less affected by mass-transfer processes.

The self-humidifying function in the PEMFC stack is less efficient if the temperature is low. This assumption has been tested with various humidity levels at 10°C. Each of the humidity experiments was obtained with at least a 6 h time-interval between tests, because self-heating occurred after each measurement, and this might change the temperature of the stack, and cause poor reproducibility.

Fig. 5a shows the experimental potential–current and power–current curves for the PEMFC stack at different humidities and at a constant temperature of 10°C. As expected, the stack voltage as shown on the potential–current curves, decreases significantly with lowering humidity. For example, at 25% r.h., the PEMFC stack cannot work properly having an open-voltage of only 18.6 V, the potential rapidly dropping to 0 V when the current reached 1 A.

Two humidity conditions, 35% and 80% r.h., were selected for electrode kinetic analysis. Fig. 5b shows the potential–current and power–current curves at these humidities. At currents smaller than 6.5 A, the calculated curves and experimental data fit excellently for the 80% r.h. condition. However, because self-heating occurred during measurement, which increased the stack's inner temperature, the data fit is poor when the current was more than 6.5 A. For humidities of 80% and 35% r.h. the values of peak power are 143.7 W at 9.9 A and 32.1 W at 1.85 A, respectively. The kinetic and mass-transfer parameters were

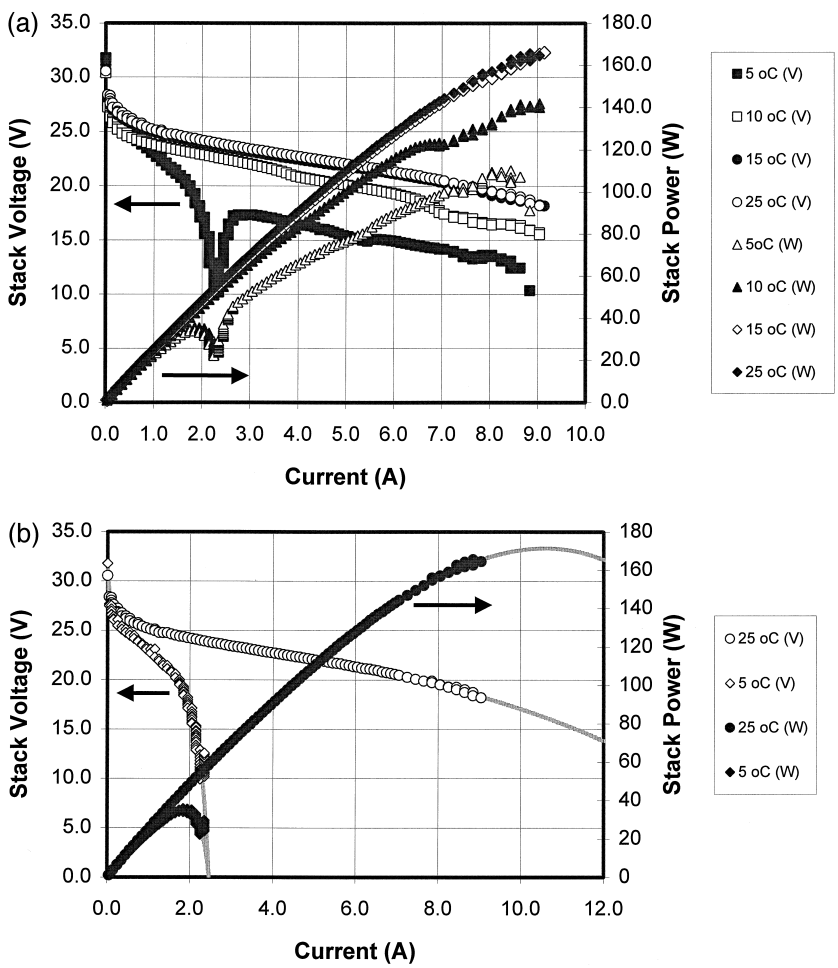

Fig. 6. (a) Effect of temperatures between 5 and 25°C on the operating voltage and power output of the 100 W PEMFC stack at a constant relative humidity of 80% r.h. (b) Effect of temperature on the operating voltage and power output of the 100 W PEMFC stack at a constant relative humidity of 80%, whereas the points are experimental data and the extrapolated curves were computed from an empirical equation.

computed for these two humidities and are shown in Table 4.

The R value at 35% r.h. is much larger than that at 80% r.h. Apparently, the low humidity causes stack resistance to increase significantly at 10°C. The n value is much larger, the i_d value is smaller and the m value is bigger at 35% r.h. than that at 80% r.h., which indicates a poor mass-transfer process for these low humidity conditions. Why the effect of humidity on the stack's performance is more apparent at 10°C than at 30°C? Because it is more difficult for the accumulated H_2O to evaporate at the lower temperature. At temperature below 10°C, the air blown through the stack's chamber contains little water, so the stack loses its self-humidifying capability.

3.2.3. Effect of temperature

Fig. 6a shows the effect of temperature on the performance of the PEMFC stack. In order to obtain reproducible results each experiment was conducted after the temperature had been equilibrated for at least 6 h. The initial rapid voltage drop at the very small current range on the potential–current curves stems from an electrode activation process, while the middle parts are controlled by ohmic processes. A slight mass transfer behaviour can be seen on these curves at the higher currents. The highest power (around 165 W) was obtained at about 9 A for temperatures of 15 and 25°C.

However, at lower temperatures, the potential–current and power–current curves are not smooth because the temperature of the inner stack fluctuated as the current passed through it. At the lowest test temperature of 5°C, the inner parts of the stack warmed up significantly with time during discharge, causing the inner temperature to go far above 5°C. Therefore, the potential–current and power–current curves rise significantly when current was more than about 2.5 A. This phenomenon is attributed to the formation at the higher currents of a new heat-exchange balance system between the stack and the environment.

Table 5
Electrode-kinetic and mass-transfer parameters for the 100 W PEMFC stack at different temperatures and at a constant relative humidity of 80%

Temperature, °C	E_0, V	b, mV dec^{-1}	R, Ω	m, Ω	n, A^{-1}	i_d, A
25	32.0	2100	0.44	0.30	0.15	6.04
5	31.0	1900	2.40	0.22	3.50	1.25

Analysis of the electrode kinetic process was completed by computer simulation. Fig. 6b shows the experimental and computed potential–current and power–current curves using Eq. (3), at different temperatures. The lines and points in the figure represent the simulated curves and experimental data, respectively. At 25°C, the all experimental points fit excellently, however, at 5°C, only the initial part of the experimental data (currents less than 2.5 A) has a good fit with calculated. There are peaks on both power–current curves. For the temperature of 25 and 5°C, the values of peak power are 171.4 W at 10.6 A and 35.7 W at 1.95 A, respectively. The kinetic and mass-transfer parameters at the two temperatures are shown in Table 5. At the lower temperature the R value is significantly larger, which reflects the decrease in ionic conductivity of Nafion membrane. The i_d value is much smaller and n value is much larger at 5° than at 25°C, which implies that a poorer mass-transfer process occurs at the lower temperature.

3.2.4. Performance over a long period

The performance of the PEMFC stack was evaluated over a long operating time. Fig. 7 shows the plot of voltage versus time for the PEMFC stack at a constant current discharge of 7.0 A for 6 h. During the first 4 h the

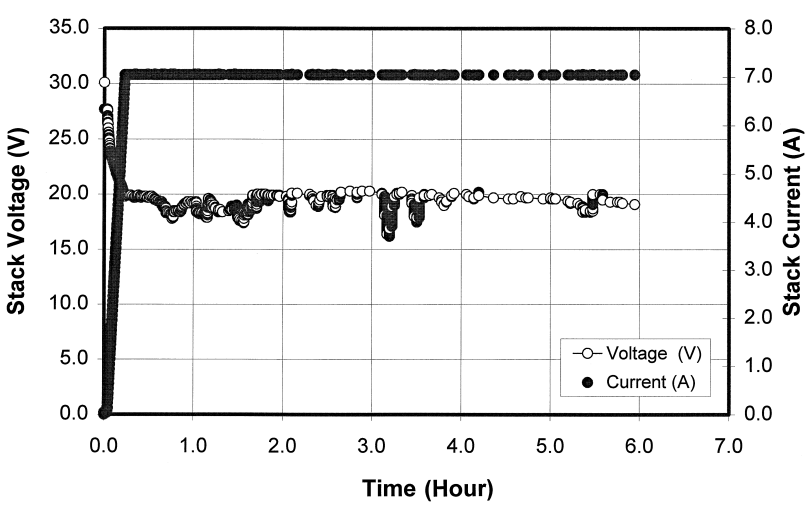

Fig. 7. Constant current discharge performance of the 100 W PEMFC stack. The current was increased gradually at the beginning, then kept constant.

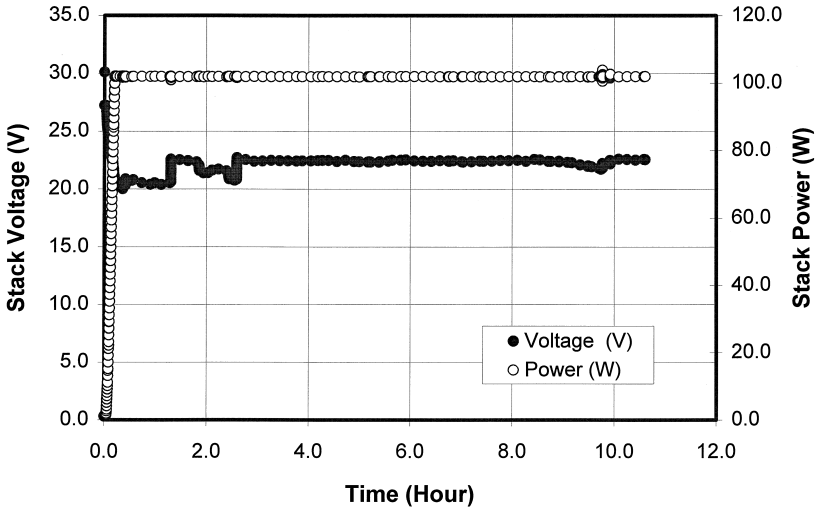

Fig. 8. Constant power discharge performance of the 100 W PEMFC stack. The power was increased gradually at the beginning to 100 W, then kept constant.

voltage fluctuated. However, after this time, the voltage remained constant at about 20 V. Because of many factors, such as electrode activation, heat-exchange, mass-transfer and humidifying, more time is required for equilibrium within the 30-cell PEMFC stack, and the optimal performance is obtained only after operation for several hours. Fig. 8 shows a constant power (100 W) discharge of the PEMFC stack for 10 h. After operation for 3 h, the output becomes constant, and the plot of voltage against time is smooth. The two experiments described above have demonstrated that the 30-cell PEMFC stack can work continuously for a long time.

During the hours of operation, a lot of water was produced, which was collected continuously in the stack's chamber, and taken out for analysis. Fig. 9 shows the water production during constant power discharge. Only about 66% of theoretical water was collected. The rest—34%—might have been lost by evaporation and blown into the environment by the cooling and oxidant fans. The water blown out by the oxidant fan plays an important role in self-humidifying the PEMFC stack.

4. Conclusion

Nafion membrane, used as electrolyte, plays an important role in the construction of PEMFC's membrane-electrode assembly (MEA). Various types of Nafion membranes, such as Nafion 117, 115, 112, 105, were tested within a single cell at different temperatures. The Nafion 112 gave the best result (0.72 V at 1.0 A cm^{-2}). A 30-cell, 100 W stack was evaluated at different humidities and temperatures. The potential–current and power–current curves both for the single cell and the stack were

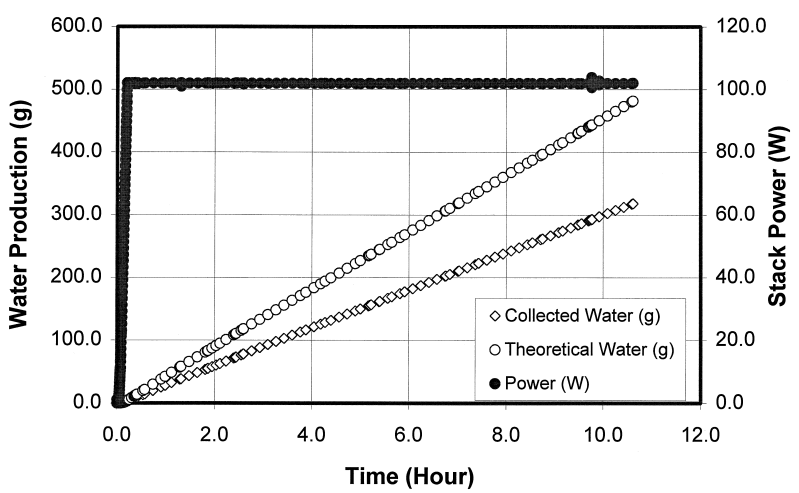

Fig. 9. Water production during a constant power discharge of the 100 W PEMFC Stack. The power was increased gradually at the beginning to 100 W, then kept constant.

analyzed by computer simulation, and kinetic and mass-transfer parameters were calculated. The open-circuit potential, Tafel slope and the d.c. resistance of the series-connected cell stack seem to be an addition of the values of the individual cells. However, the mass-transfer behaviour of the stack is more complicated, compared with the single cell because of the presence of other factors, such as heat-exchange, humidity effects as well as air and fuel supplies. The long-term performance of the stack and the water production during long-term operation were also measured. The stack-system becomes more stable and gives optimal performance after several hours of running under constant current or constant power, and the maximum power (ca. 170 W) of the stack is then obtainable. Only 66% of the theoretical water produced was actually collected during long-term operation, while the other 34% was lost by evaporation. Self-humidifying was achieved by employing the water produced from the cathode electrode. Self-humidifying is more efficient at 30°C than at temperatures of 10°C and below.

Acknowledgements

The authors wish to thank the Army Materiel Command for its financial support of this project.

References

[1] T.F. Fuller, The Electrochemical Society Interface, Fall 1997, p. 26.
[2] E.A. Ticianelli, C.R. Derouin, S. Srinivasan, J. Electroanal. Chem. 251 (1988) 175.
[3] I.D. Raistrick, U.S. Patent 4,876,115 (1990).
[4] M.S. Wilson, S. Gottesfeld, J. Appl. Electrochem. 22 (1992) 1.
[5] J. Kim, S.M. Lee, Srinivason, C.E. Chamberlin, J. Electrochem. Soc. 142 (1995) 2670.
[6] Y.W. Rho, O.A. Velev, S. Srinivason, Y.T. Kho, J. Electrochem. Soc. 141 (1994) 2084.
[7] H.F. OetJen, V.M. Schmidt, U. Stimming, F. Trila, J. Electrochem. Soc. 143 (1996) 3838.
[8] M. Uchida, Y. Aoyama, N. Eda, A. Ohta, J. Electrochem. Soc. 142 (1995) 4143.
[9] F.N. Buchi, B. Gupta, O. Haas, G.G. Scherer, J. Electrochem. Soc. 142 (1995) 3044.
[10] M. Uchida, Y. Aoyama, N. Eda, A. Ohta, J. Electrochem. Soc. 142 (1995) 463.
[11] J.B. Lakeman, J. Cruickshank, Proc. 38th Power Sources Conference, 1998, Cherry Hill, NJ, p. 420.
[12] A.C. Oliver, E. Clarke, Proc. 38th Power Sources Conference, 1998, Cherry Hill, NJ, p. 424.
[13] L.P. Jarvice, D. Chu, Proc. 38th Power Sources Conference, 1998, Cherry Hill, NJ, p. 428.
[14] O. Polevaya, D. Bloomfield, Proc. 38th Power Sources Conference, 1998, Cherry Hill, NJ, p. 416.